The shape memory properties of multi-layer graphene reinforced poly(L-lactide-co--caprolactone) by an atomistic investigation

IOP Publishing Smart Materials and Structures
Smart Mater. Struct. **30** (2021) 055005 (10pp) https://doi.org/10.1088/1361-665X/abeef9

The shape memory properties of multi-layer graphene reinforced poly(L-lactide-co-ε-caprolactone) by an atomistic investigation

Xue-Jiao Zhang[1], Qing-Sheng Yang[1,*], Jun-Jun Shang[1], Xia Liu[1] and Jin-song Leng[1,2]

[1] Department of Engineering Mechanics, Beijing University of Technology, Beijing 100124, People's Republic of China
[2] Center for Composite Materials and Structures, Harbin Institute of Technology, Harbin 150001, People's Republic of China

E-mail: qsyang@bjut.edu.cn

Received 19 October 2020, revised 8 February 2021
Accepted for publication 15 March 2021
Published 26 March 2021

Abstract

In this paper, an atomistic investigation was performed to reveal the dependence of the graphene content on the shape memory effect of the multilayer graphene reinforced poly (L-lactide-co-ε-caprolactone). Uniaxial compression deformation was carried out to show the shape memory effect of the graphene composites. The temperature response of the composites was obtained during shape recovery. It is observed that the composites with higher graphene content exhibit larger recovery ratio and are more sensitive to temperature during a gradual warming recovery. The graphene composites show good reusable properties and the shape of composites is able to fully recover by constant temperature recovery tests. Especially, the graphene of the composite was subjected to a separate heating test to check the role of the graphene in shape recovery of the composite, where electro-induced indirect heating was qualitatively simulated. It is shown that the recovery first appeared in composites with the most content of graphene. The polymer will have a temperature hysteresis compared with graphene in composites. The shape recovery trajectory of graphene and the evolution of the interaction between graphene and polymers during the process of shape memory were clearly presented to reveal the mechanism how graphene promotes the performance of shape memory. This research can provide a guidance for obtaining composite materials with ideal shape memory effect.

Keywords: polymer composites, graphene content, layered structures, shape memory effect, atomistic simulation

(Some figures may appear in colour only in the online journal)

1. Introduction

Among smart materials, stimulus responsive shape memory polymers (SMPs) have good application prospects. They can change their shape and characteristics through changes in external conditions such as light [1, 2], temperature [3], pH [4, 5], electricity [6] and magnetic field [7]. There exist many attractive features such as large elastic range, large recovery strain, light weight, easy processing and low cost on SMPs [8]. Some of them have good transparency, strong chemical stability, and biocompatibility which can adjust the degradation rate [9]. Furthermore, SMPs respond to a wide range of stimuli. Direct heating is the most common method to trigger

* Author to whom any correspondence should be addressed.

SMPs. The shape memory function is mainly derived from the two-phase structure existing in the material. A stationary phase (covalent or physical cross-linking) that maintains the shape at temperature below transition temperature (glass transition temperature T_g or melting temperature T_m). A reversible phase (crystallization, chemical cross-linking) that changes reversibly with environmental changes above transition temperature [10]. These heating methods may not be suitable for all situations, such as *in vivo* and aerospace devices. A direct method of indirect heating is electric heating. When conductive fillers are added to SMPs, the internal joule heat can indirectly drive the shape memory effect.

Graphene nanoplatelets with excellent electrical conductivity, ultra-high elasticity modulus, high specific surface area and aspect ratio [11] make graphene an ideal filler for polymer composites. They cause significant thermal and electrical activation of the shape memory response to the matrix [12, 13]. Dynamic mechanical analysis showed that the inclusion of graphene significantly improves both glassy and rubbery moduli of the matrix. Furthermore, the prepared nanocomposites demonstrated a marked electrical conductivity and thereby surprisingly rapid electrical actuation behavior exhibiting a 100% recovery ratio in 2.5 s [14]. With the increment of graphene nanosheets content, the modulus is increased. The calculation of shape memory properties showed that shape fixity and shape recovery ratios also increased with increasing of incorporating of graphene nanosheets [15]. Graphene content is a very important factor to the mechanical properties and shape memory properties of polymers. Addition of graphene also can improved thermal stability of the polymer nanocomposites. The results of multiple thermal cycles show that a larger viscous plastic deformation was observed when neat polyimide is under stress at high temperature compared to graphene nanocomposites. The recovery rate of graphene nanocomposites is higher than that of pure polymers [16]. However, the underlying mechanism of graphene properties in SMP composites remains mystical. It is difficult to determine the interaction between graphene and polymer in experiments. Analysis should be performed to determine the effect of graphene content on overall shape memory performance, and to evaluate the thermo mechanical properties and microstructure of the resulting nanocomposites.

The molecular dynamics (MD) method is a promising tool to predict the thermodynamic properties of composites. Sarangapani *et al* [17] simulated specific volume of different amorphous polymeric models to exhibit a characteristic change when amorphous systems change from glassy to rubbery state by MD simulations. Choi [18] discussed the effect of filler size on the glass transition and thermoelastic behavior of epoxy-based nanocomposites. Wang [19] studied the glass transition behavior and mechanical properties of poly(ethyleneterephthalate) (PET) and its nanocomposites through MD simulation. Li investigated miscibility, glass transition temperature and mechanical properties of polymethyl methacrylate (PMMA) and dibutyl phthalate (DBP) binary system by MD simulation [20]. The Young's modulus and shear modulus of the composites with different graphene volume fractions under different temperatures are simulated and discussed by Lin [21]. The results show that the Young's and shear moduli increase with the increase of graphene volume fraction and have temperature dependence. MD simulation can reliably study the physical and mechanical properties of polymers and their nanocomposites. Diani [22] studied the shape memory behavior of polyisoprene under uniaxial tension loading using full atom simulations. The results of strain storage and energy evolution show that shape memory behavior is driven by entropy. Ghobadi *et al* [23] established an atomic model of poly(*L*-lactide) to predict the uniaxial stretch shape memory behavior, and described two simulations using Parinello–Rahman stretch and geometric stretch simulation methods. Aberton [24] proved the influence of phase fraction and temperature on the shape recovery of the copolymer system by using a coarse-grained molecular model. The dependence of shape memory on molecular weight of polymer was studied by Zhang [25]. The results show that repeated stretching can improve the recovery rate of the polymer. Moon [26] investigated the effect of initial strain on the thermo elasticity and shape recovery behavior of oriented polystyrene. It was found that the anisotropy of linear thermal expansion coefficient and elastic modulus mainly increased with the increase of pre-stretching. However, the above comprehensive researches mainly focused on the effect of deformation loading conditions on SMPs. Zhang [27] studied the strength and shape memory properties of polymer composites consisting of graphene sheets in different directions, and there are covalent bonds between graphene and polymers. The interaction between filler and polymer on shape memory composites is complex. The content of graphene has a great influence on the properties of SMPs. Few studies have reported the action mechanism of graphene in SMP composites at microscopic scale and it is very necessary to study this issue.

In this paper, the properties of SMPs and their multi-layer graphene reinforced composites have been studied from the microscopic point of view by MD method. Uniaxial compression of composites including different content of continuous graphene has been investigated. The effect of graphene addition on the properties of SMPs was revealed. The shape memory effect of materials was demonstrated to observe shape response of SMP to temperature by different heat methods during shape recovery. The shape recovery trajectory of graphene was clearly presented. The evolution of the interaction between graphene and polymers during the process of shape memory contributed to explore the mechanism how graphene promotes the performance of shape memory from an energy perspective.

2. MD models and simulation processes

Initial amorphous cells of poly (*L*-lactide-co-ε-caprolactone), PCLA, were established referenced the former research [27]. The MD simulations were employed with the LAMMPS program developed by Sandia National Laboratory [28]. The PCFF force field [29] was used to describe the covalent and non-bonding interactions between atoms. The non-bonding interactions were neglected when the distance is larger

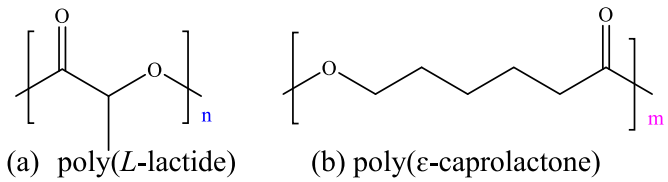

Figure 1. Chemical formula of poly(*L*-lactide) and poly(ε-caprolactone).

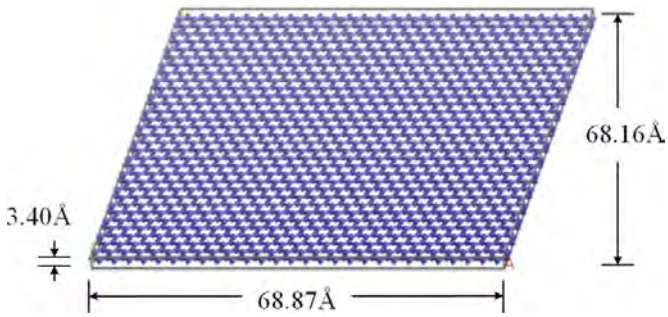

Figure 2. Graphene sheet model.

than 12.5 Å. All the simulations are performed under periodic boundary conditions. The models were conducted to optimized structures by relaxation processes. The parameters for each simulation are given below.

2.1. Establishment of PCLA composites

The chemical formulas of poly(*L*-lactide) and poly (ε-caprolactone) are shown in figures 1(a) and (b). Each chain consists of 50 repeating units, including poly (*L*-lactide) and poly(ε-caprolactone). The ratio of repeating unit poly(*L*-lactide) to poly(ε-caprolactone) is 6:4. Each model contains 44 PCLA chains. The side length of pure polymer box is 68.83 Å. The size of the graphene sheet is 68.87 × 68.16 Å as shown in figure 2, and the thickness of single sheet is 3.40 Å. The height of the composite model with single layer graphene is 69.96 Å, the height of the bilayer graphene composite model is 73.36 Å, and the height of the tri-layer graphene composite model is 76.76 Å. The volume fraction is determined by the thickness of the graphene sheets relative to the overall height of the model. The volume fraction of graphene in the polymer composites are 4.86 vol.%, 9.27 vol.% and 13.29 vol.%, respectively. Figure 3 shows composite models with graphene in the center of the model. The three models are called Com#1, Com#2, and Com#3. The initial density is 1.0 g cm^{-3}. The model is subjected to energy minimization and relaxation for 1 ns at 410 K, 0.1 MPa under NPT ensemble.

2.2. Glassy state and rubber state for materials

Glass transition temperature T_g is a physical characteristics of the amorphous polymer translating from a glassy state to a rubber state. Since the viscoelasticity of the polymer is greatly sensitive to temperature near T_g, T_g is popularly used as the reference standard. Differential scanning calorimetry is often used in experiments to determine T_g of nanocomposites. The glass transition temperature range of PCLA obtained by copolymerization of poly(*L*-lactide) and poly (ε-caprolactone) in different proportions was different, and the T_g of poly(*L*-lactide)/poly(ε-caprolactone) 6:4 copolymer is 287 K by experiments [30]. It is stated that the glass transition temperature of pure polymer moved toward a higher temperature after graphene oxide filling is increased [31]. In our previous study, the glass conversion temperature of pure PCLA was 280–290 K, and T_g of polymer added graphene was about 10–20 K higher than that in the pure polymer [27]. Since MD simulation can only predict the glass conversion temperature within a certain range, models with different graphene content may have similar temperatures. Instead of predicting the transformation temperature, glass state and rubber state were chosen for comparison in this part.

The mean square displacement (MSD) was used to show activation of atoms. The MSD curves of the PCLA chains can be obtained

$$\mathrm{MSD} = \sum_{i=1}^{N} \left\langle |r_i(t) - r_i(0)|^2 \right\rangle \tag{1}$$

where, $r_i(t)$ is the position of the atom i at time t, and N is the number of atoms in the system.

The high temperature of $T_h = 410$ K and the low temperature of $T_l = 250$ K were selected as the representative temperatures of glass state and rubber state, and the MSD was calculated to observe the atomic activities. The relaxed structure is set to the representative temperatures and 0.1 MPa at NPT ensemble for 500 ps. It can be seen from figure 4 that the MSD value of composite material at T_h is much lower than that of pure polymer, indicating that graphene has an inhibitory effect on polymer chain activity. At low temperature, there is little difference between pure polymers and composites, and Com#3 has slightly more activity than others.

2.3. Shape memory process description

The thermo-mechanical cycle was simulated to explore the shape memory effect of composites. Uniaxial compression parallel to the graphene direction was performed on composites. The simulation process of the shape memory cycle for composite is shown in figure 5. The thermo-mechanical cycle includes four steps: (a) uniaxial compression of the material above T_g; (b) maintaining the deformation and cooling below T_g; (c) unloading at low temperature; (d) the temperature rises above T_g again to observe the shape recovery.

First step, compress the relaxed materials at standard atmospheric pressure and high temperature of $T_h = 410$ K (above T_g) under the NPT ensemble to the strain of $\varepsilon_l = 50\%$; in the cooling step, NVT ensemble was used to keep the material in deformed state, and then cool it at $T_l = 250$ K (below T_g). Since the pressure in the system cannot be released at low temperatures, we use an NPT ensemble to release the internal stress of the material, the strain is ε_u after unloading. Finally,

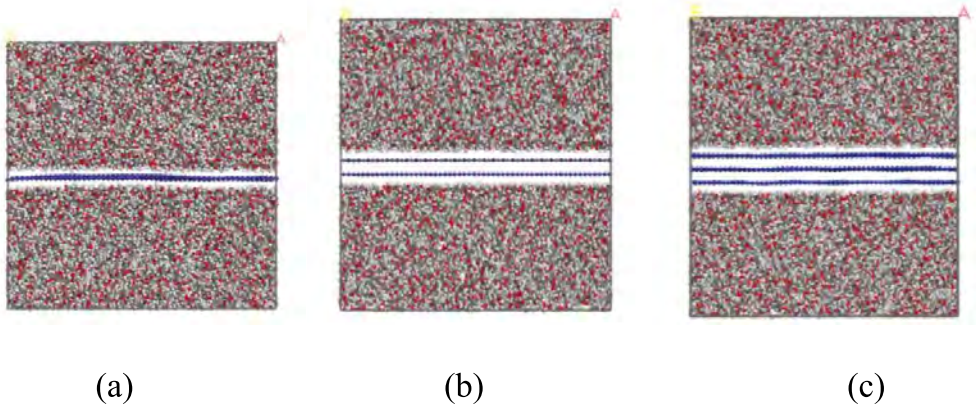

Figure 3. The models of graphene enforced PCLA composite. (a) Com#1; (2) Com#2, and (c) Com#3.

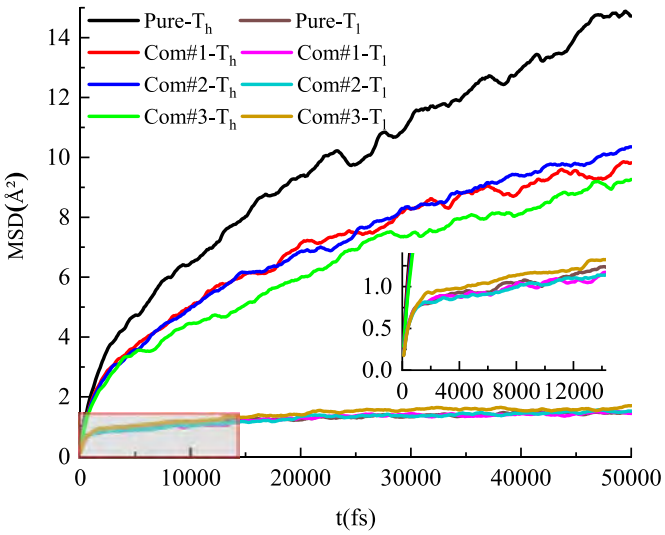

Figure 4. The MSD curves of pure PCLA and graphene enforced PCLA composite.

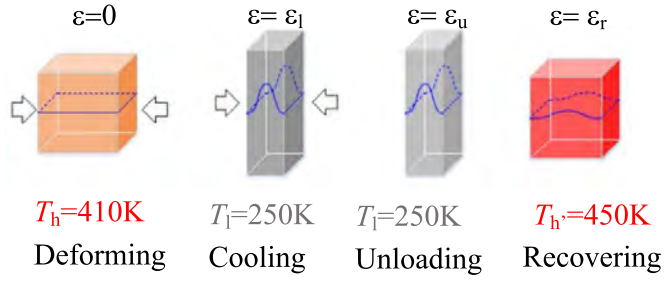

Figure 5. The thermo mechnical cycle of graphene composites.

increase the system temperature T_h' above T_g under the NPT ensemble, and the final strain was ε_r. In the follow-up test, three ways of heating to recover the shape were used. T_h' was set to 450 K in the constant temperature recovery method, and T_h' was in range of 250 K to 450 K in the gradual heating recovery method and individual heating of graphene method. When the graphene in the composite was heated separately, the NVE ensemble was used to refresh the velocity and location of polymer atoms, and the graphene sheets were controlled under the NPT ensemble.

$$\varepsilon_x(t) = \frac{l_x(t) - l_0}{l_0} \tag{2}$$

where, l_0 is the original length of the simulation box for the deform direction and $l_x(t)$ represents the length of the simulation box for the deform direction at time t.

The virial stress is commonly used to connect the macroscopic (continuum) stress [32, 33]. The components of the macroscopic stress tensor, σ_{ij}, in a volume Ω is

$$S_{ij} = \frac{1}{\Omega}\sum_{a\in\Omega}\left[-m^{(a)}v_i^{(a)}v_j^{(a)} + \frac{1}{2}\sum_{b\in\Omega}((r_i^{(a)} - r_j^{(b)})F_j^{(ab)})\right] \tag{3}$$

which generates the six components of the symmetric stress volume tensor S_{ij}. $m^{(a)}$ is the mass of particle 'a', $v_i^{(a)}$ and $v_j^{(a)}$ are velocities for the ith and jth vector component basis, $r_i^{(a)} - r_j^{(b)}$ represents the distance between particle 'a' and atom 'b' along the ith vector component, and $F_j^{(ab)}$ represents the force on particle 'a' exerted by particle 'b' along the jth vector component, and Ω is the volume. The total stress can be expressed as

$$\sigma_{ij} = S_{ij}\Omega^{-1} \tag{4}$$

where Ω is the volume of materials at the periodic boundary condition.

3. Results and discussion

3.1. Response to temperature during recovering

The response of thermo-sensitive SMPs to temperature is the key to ensuring their shape memory performance. Shape fixing ratio R_f and recovery ratio R_r are important indexes to measure shape memory effect, which can be obtained from equation (5).

$$R_f = \frac{\varepsilon_u}{\varepsilon_l}, \quad R_r = \frac{\varepsilon_l - \varepsilon_r}{\varepsilon_l}. \tag{5}$$

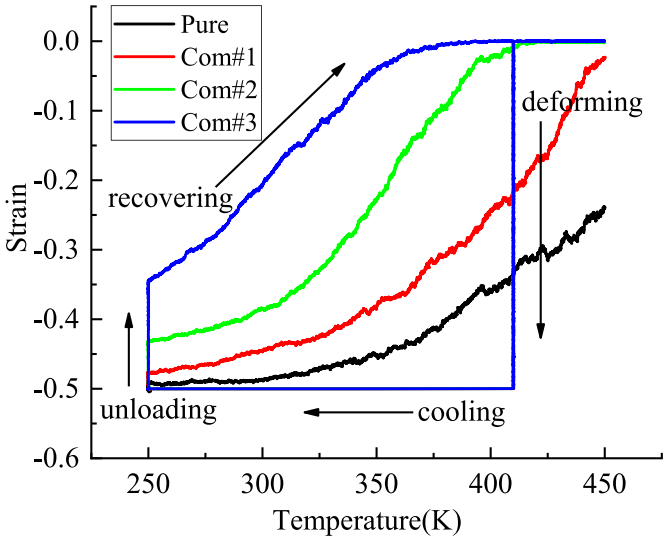

Figure 6. The relationship between temperature and strain of pure polymer and composites.

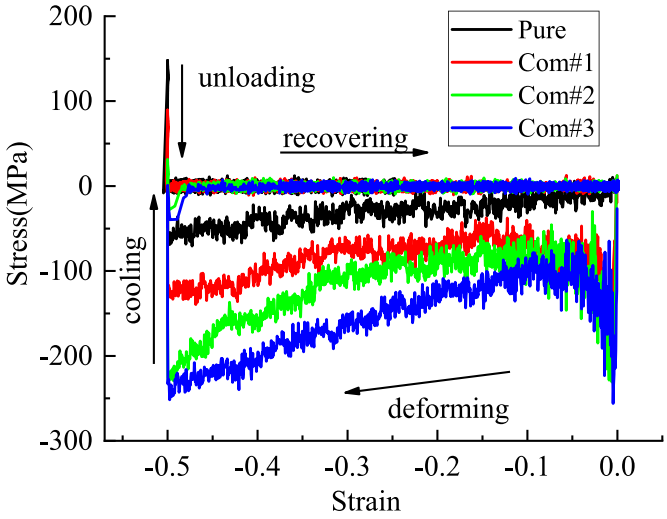

Figure 7. Stress–strain relationship of pure polymer and composites.

Figure 6 shows the stress state when the temperature of polymer and its composite changes during shape memory. Gradually heat up all the materials in the recovery step. All materials were compressed at a temperature of 410 K and deformed 50% from the strain of 0, then kept deformed at a cooling temperature of 250 K. The curves of all the materials in these two steps coincide perfectly. When unloading is carried out at 250 K, the curves of each material show obvious differences. With the increase of graphene content, the unloading line segment becomes longer, which means that the recovery of strain in unloading changed more greatly. It is calculated that the fixing ratio of pure polymer is 98.42%, and the fixing ratio of composite material is 95.22%, 86.36%, 68.96%, respectively. As the graphene content increases, the fixing ratio becomes worse. It can be found the recovery of each material shows an upward trend with the increase of recovery temperature. Among them, Com#3 has the fastest recovery speed, and the recovery is completed first. The shape of Com#1 and Pure have not fully recovered. By comparison, it can be concluded that the graphene composites have a rapid response to temperature.

The stress–strain relationship of each material under thermodynamic cycles is shown in figure 7. At the initial moment, all material stresses are zero. Here the minus signs for stress and strain indicate deforming direction rather than magnitude. As loading was beginning, the stress values of the three composite materials increased rapidly, and the stress values of Com#2 and Com#3 reached more than 200 MPa, and Com#3's stress was slightly larger than that of Com#2. Then the stress of composites drops until the strain exceeds 5%. Then the decreasing stress begins to increase with the strain the deformation. The stress of the pure polymer model increases with the deformation all the way. The increasing of modulus and strength leads to the increased area under the curve which is the elastic strain energy stored in samples and acts as shape recovery driving force in shape memory cycles [34]. Here, the material is compressed, and the recovery driving force is the area bounded by the 0 axis and the curve below it. Com#3 has the greatest elastic strain energy and shape recovery driving force in all material.

3.2. Reusable property

Graphene composite has been reported to have high recovery ratio and superior reusability [16]. Three thermo-mechanical cycle tests were carried out to the material where shape recovery took place at the constant temperature. In order to compare with the result of section 3.1, the constant temperature was 450 K. The fixed strain ratios and recovery ratios of materials in three cycles are shown in table 1. Three cycles of each material have stable performance. The fixing ratio of pure polymer is above 98.00%. Com#1 has the best fixing ratio among the composite materials, which is above 95.00% all three times. As the content of graphene increases, the fixing performance of the composite material is greatly reduced. While the recovery ratio of the three graphene composite materials is over 99% each time from the recovery performance.

Figure 8 shows in detail the corresponding relationship of strain and temperature at each step of the first cycle. Figures 9 and 10 show the strain and stress changes in the three cycles, respectively. And the duration of each step in each cycle is the same as in figure 8. At the same recovery temperature, the composites recovered their deformation in a short time. The recovery rate is getting slow at a small strain. The addition of graphene not only improves the material recovery ratio, but also greatly improves the recovery rate. The change trend of stress and strain in the three cycles were consistent, which reflect the stability of the compressive shape recovery.

3.3. Research on individual heating of graphene in polymer

A method of indirect heating for shape memory material is electric heating. When graphene is added to SMPs, the

Table 1. Shape memory properties of polymers and their composites.

	Cycle 1		Cycle 2		Cycle 3	
%	Fix ratio	Recovery ratio	Fix ratio	Recovery ratio	Fix ratio	Recovery ratio
Pure	98.42	72.44	99.24	78.24	99.76	69.12
Com#1	95.22	99.86	96.80	99.84	97.48	100.00
Com#2	86.36	99.80	85.50	99.90	91.18	99.90
Com#3	68.96	99.94	65.26	99.96	69.18	99.96

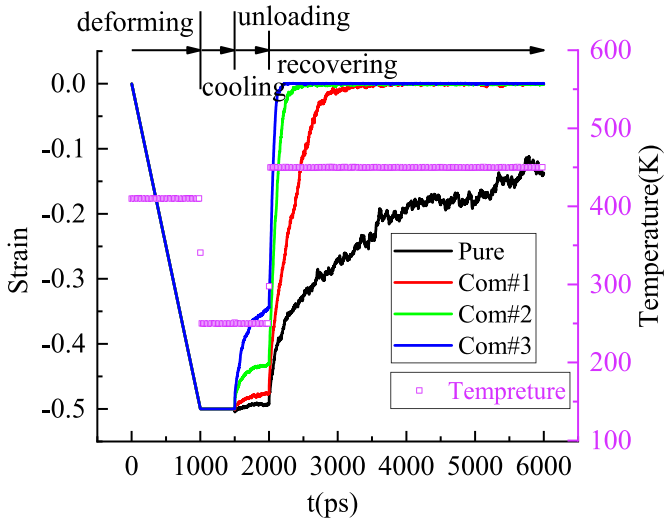

Figure 8. Temperature and strain change on thermo mechanical cycle.

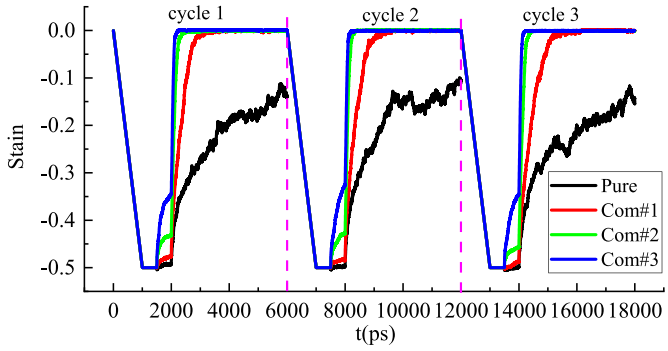

Figure 9. Strain change on three times of thermo mechanical cycle.

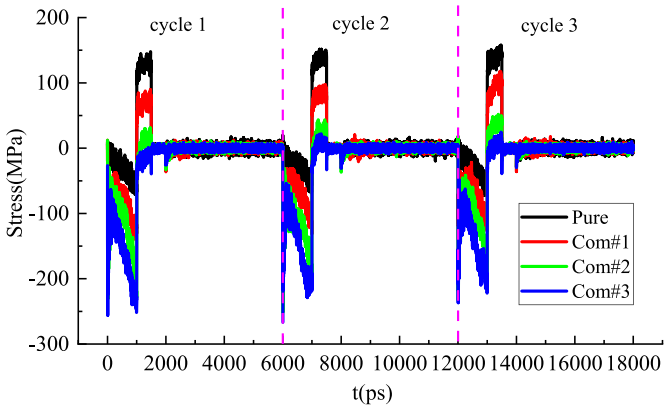

Figure 10. Stress change on three times of thermo mechanical cycle.

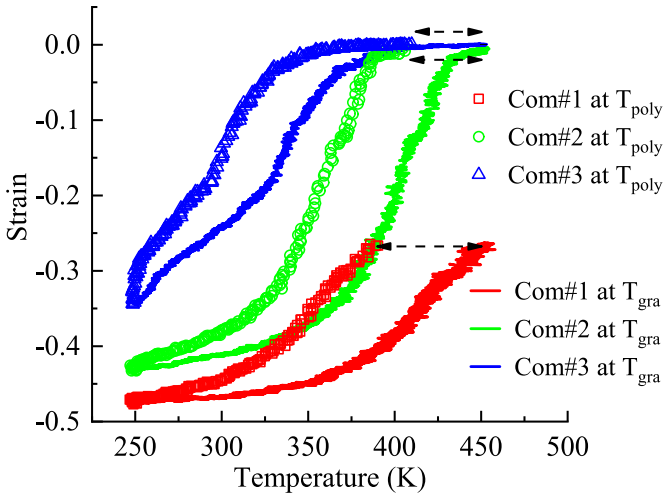

Figure 11. Temperature strain relationship of composites.

internal joule heat generated can indirectly drive the shape memory effect. The graphene content in the polymer exceeds a certain percolation threshold and starts to conduct electricity. The heat generation for one material is determined by the applied voltage and time. While for different materials, the resistance affects the rate of heat generation. Different amounts of graphene correspond to different electrical resistance. The increase of graphene content will decrease the resistance. Therefore, graphene of composites is individually heated to simulate the situation of electric heating. The graphene is heated separately from 250 K to 450 K at 50 K ns^{-1}. The heating rates of the three composites were set to be the same as applying the same voltage and time. So the heat of graphene depends on its content, the shape of the material with high graphene content will recover quickly. Figure 11 shows the temperature of the composite in the recovery step, and the same strain corresponds to the same time. It can be seen that the polymer temperature rises accordingly, and there is a hysteresis section relative to graphene. The lower the graphene content, the more obvious the temperature hysteresis.

It is calculated that the recovery ratio of composite material is 47.52%, 99.20%, 100.10% with graphene content increase, respectively. Looking at the deformation diagrams at important steps of the thermodynamic cycle in figures 12–14, it can be found that graphene bent during the deformation process. Buckling of graphene occurs. Based on table 2 and

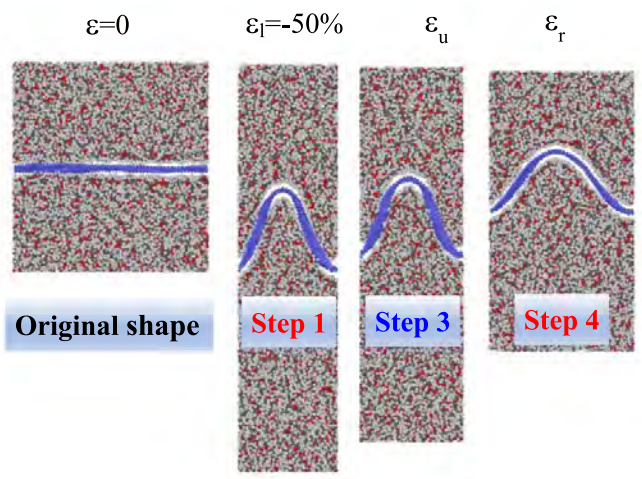

Figure 12. Shape memory and graphene recovery trajectory of the single-layer graphene model.

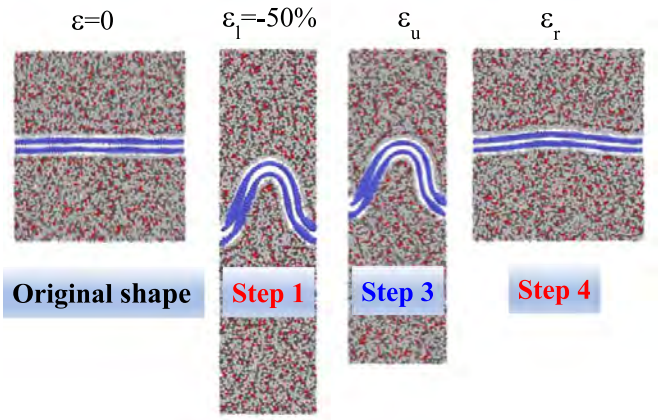

Figure 13. Shape memory and graphene recovery trajectory of the double-layer graphene model.

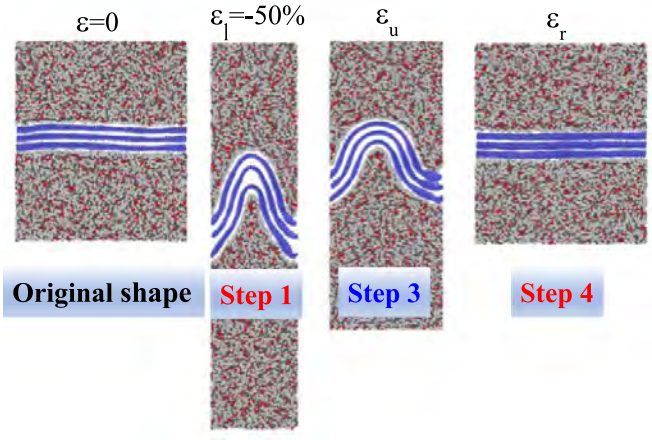

Figure 14. Shape memory and graphene recovery trajectory of the three-layer graphene model.

figures 12–14, the shape of graphene also recovers when the shape of the composite recovers. So the buckling deformation of graphene in all composites can recover completely with sufficient time and temperature, since all composites recover completely during the thermo-mechanical cycles in section 3.2. It can be found that the elastic buckling deformation of graphene hinders the shape fixation of SMP, and provides a certain driving force for the shape recovery of SMP. The change of the graphene bending angle indicates the degree of recovery. A schematic diagram of the deformation angle of graphene in the polymer is shown in figure 15. During the whole thermo-mechanical cycle, the highest and lowest position atoms at the moment of maximum deformation were record. The choice of representative layers is the lamellae in contact with the polymer. The highest and lowest position atoms were chosen at the second layer of graphene for the Com#2. The represented atoms were marked at the third layer of graphene for Com·#3. The angle change of the highest atom in the subsequent recovery process is obtained, and the calculation is as follows:

$$\tan\theta(t) = \frac{Z_{\max}(t) - Z_{\min}(t)}{X_{\max}(t) - X_{\min}(t)} \tag{6}$$

where θ is the angle between x direction and the line connecting the highest and the lowest atom, $Z_{\max}(t)$ and $Z_{\min}(t)$ are the location of the highest and lowest atoms in the z direction, respectively. $X_{\max}(t)$ and $X_{\min}(t)$ are the location of the highest and lowest atoms in x direction, respectively.

Table 2 lists the angleθ of the graphene sheet from the moment of maximum deformation to the recovery step. When $T = 1$ ns, the graphene sheet is at the moment of maximum deformation; when $T = 2$ ns, it is the shape after unloading; when $T = 3$–6 ns, it is in the process of recovery. The shape change trajectory diagram shows the process of graphene from maximum deformation to completion of recovery in each material, and the orange trajectory is the shape from maximum deformation to completion of unloading. The shape change in the recovery trajectory is marked as the light blue trajectory. The dark particles are graphene sheets.

It can be seen in table 2 that at the maximum deformation, as the graphene content increases, the deformation angle increases. Combined with figures 12–14, it is found that the polymer around graphene decreases with increasing content. When the load is removed, the tri-layer graphene in Com#3 rebounds quickly, the deformation angle decreases, and the shape recovery intensifies. Comparing the rate of angle change in the recovery step, it can also be intuitively felt that the tri-layer graphene responds more quickly to temperature. The trajectory map shows that monolayer graphene deformed and recovered most smoothly. Tri-layer graphene experienced a shape fluctuation from maximum deformation to recovery. The possible reason is that the elastic energy of different graphene layers is different, which leads to the inconsistency of deformation.

In order to clarify the interfacial binding properties vary at different steps of the shape memory cycle for the same material, we evaluated the interaction energy between the graphene and PCLA as follows

Table 2. Changes of graphene morphology, angle and motion trajectory.

Model	t (ns)	tanθ	Shape change trajectory
Com#1	1	1.39	
	2	1.26	
	3	1.17	
	4	1.20	
	5	1.02	
	6	0.75	
Com#2	1	1.61	
	2	1.45	
	3	1.36	
	4	1.21	
	5	0.69	
	6	0.09	
Com#3	1	1.65	
	2	1.09	
	3	0.80	
	4	0.40	
	5	0.12	
	6	−0.02	

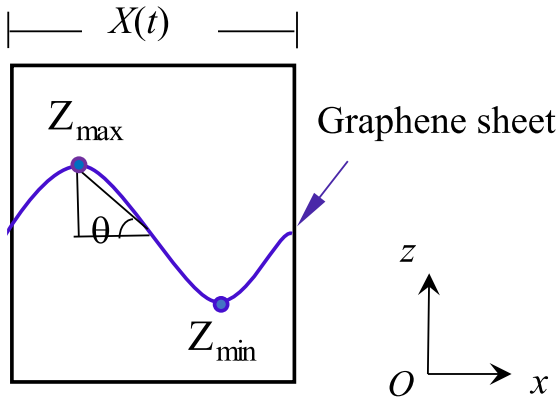

Figure 15. Schematic diagram of graphene angle calculation.

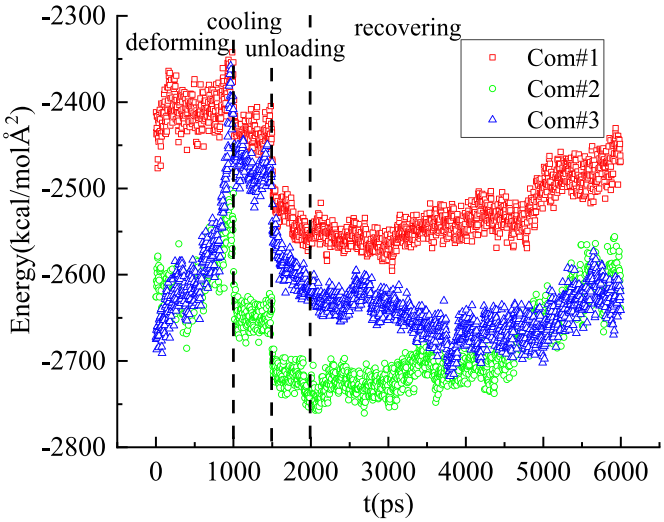

Figure 16. Interaction energy between graphene and polymer.

$$\Delta E = E_{\text{total}} - E_{\text{poly}} - E_{\text{gra}} \tag{7}$$

where ΔE is the interaction energy, E_{total} is the total potential energy of the graphene/PCLA system, E_{gra} is the potential energy of the graphene without the polymer, and E_{poly} is the potential energy of the PCLA without the graphene. Figure 16 shows the interaction energy between polymer and graphene during thermo mechanical cycle. The interaction energy is negative during each step of thermo mechanical cycle showing the existence of attractive interaction between polymer and reinforcement. The absolute value of the interaction energy determines the strength of the interaction. A large absolute value represents a strong interaction. During compression deformation, the interactions of the three composites are all decreasing. The more graphene content, the more significant the weakening interaction. By comparing figures 12–14, graphene divides the polymer into two parts. The formation of deformation increases the lamellar spacing of multilayer graphene in Step 1. The deformation angle of the composite increases with the increase of graphene content, and the area of the polymer wrapped under the curve decreases. These may cause the interaction to decrease with the graphene content. As the temperature decreases, the interaction is increased. Because the shape of cooling step is fixed, the interaction energy remains unchanged. Due to the release of internal force during the unloading step, part of the shape is restored and the interaction energy is increased. There are two situations in the final recovery step. The energy in Com#1 and Com#2 remain unchanged at the beginning. Then the temperature rises, the absolute value of energy decreases and finally reaches the value of the undeformed moment. At the beginning of the recovery step, the absolute value of energy for Com#3 first increases and then decreases that finally reaches the undeformed moment. The possible reason is that the elasticity of the tri-layer graphene is too large, and it is difficult to fix it at

high temperature where polymer is active. So this is also the reason for its poor fixing ratio.

4. Conclusion

In this paper, shape memory properties of multilayer graphene reinforced PCLA were investigated by MD method. The dependence of the shape memory and mechanical properties of the composites on the graphene content was studied by the uniaxial compression thermo-mechanical test. The whole shape memory process was demonstrated and discussed in detail. For the fixing properties, the shape memory fixing ratio decreases as the graphene content increases. For the recovery stage, different heating methods are adopted, which shows the superiority of composite materials on temperature response comparing to pure polymer. In the gradual heating recovery test, the final recovery ratio of composite has obvious difference. The recovery ratio becomes higher and the shape recovery is accelerated with graphene content increasing because composite with higher graphene content is more sensitive to temperature. When recovering at a constant high temperature, all composites containing graphene can recover completely, and the shape recovery rates of the material increased with the graphene content. The stiffness of composites are much higher than that of pure polymer from the relation of stress and strain, which means composites possess larger driving forces. Moreover, graphene was heated alone, which was regarded as a method to observe materials performance similar to electric heating recovery. The temperature of the polymer has a hysteresis compared to graphene. The hysteresis of the composites with various graphene content is different. The hysteresis is serious in composite with single layer graphene. While composites containing two or three layers graphene can be completely recovered by heating graphene only. The graphene deforming trajectory clearly demonstrates the fixing and recovery characteristics of composites containing different contents of graphene. Interactions between graphene and polymer also contribute to explain the mechanism of composites shape memory. In conclusion, the results show that the two-layer graphene composites have better fixed and recovery properties, and respond well to various reheating methods. For shape memory composite materials, the amount of graphene should be moderate, not more is better.

The paper proposed a successful simulation strategy of the shape memory properties of multilayer graphene reinforced polymers. From the aspects of deformation and energy, the shape memory mechanism of graphene composites is intuitively analyzed. This method provides us with new ideas, and the subsequent simulations before experiments will be helpful to guide the experiment.

Acknowledgments

This work is supported by the National Natural Science Foundation of China under the Project Nos. 11632005, 11772012, 11872079, and11902010 which are gratefully acknowledged.

ORCID iDs

Qing-Sheng Yang https://orcid.org/0000-0002-1621-0497
Xia Liu https://orcid.org/0000-0002-1820-4840
Jin-song Leng https://orcid.org/0000-0001-5098-9871

References

[1] Lendlein A, H Y J, Junger O and Langer R 2005 Light-induced shape-memory polymers *Nature* **434** 879–82
[2] Chatani S, Kloxin C J and Bowman C N 2014 The power of light in polymer science: photochemical processes to manipulate polymer formation, structure, and properties *Polym. Chem.* **5** 2187–201
[3] Behl M, Kratz K, Noechel U, Sauter T and Lendlein A 2013 Temperature-memory polymer actuators *Proc. Natl Acad. Sci.* **110** 12555–9
[4] Guo W, Lu C, Orbach R, Wang F, Qi X, Cecconello A, Seliktar D and Willner I 2015 pH-stimulated DNA hydrogels exhibiting shape-memory properties *Adv. Mater.* **27** 73–8
[5] Han X, Dong Z, Fan M, Liu Y, Li J, Wang Y, Yuan Q, Li B and Zhang S 2012 pH-induced shape-memory polymers *Macromol. Rapid Commun.* **33** 1055–60
[6] Lu H, Liu Y, Gou J, Leng J and Du S 2010 Electrical properties and shape-memory behavior of self-assembled carbon nanofiber nanopaper incorporated with shape-memory polymer *Smart Mater. Struct.* **19** 75021
[7] Yu X, Zhou S, Zheng X, Guo T, Xiao Y and Song B 2009 A biodegradable shape-memory nanocomposite with excellent magnetism sensitivity *Nanotechnology* **20** 235702
[8] Hu J, Zhu Y, Huang H and Lu J 2012 Recent advances in shape–memory polymers: structure, mechanism, functionality, modeling and applications *Prog. Polym. Sci.* **37** 1720–63
[9] Pilate F, Toncheva A, Dubois P and Raquez J 2016 Shape-memory polymers for multiple applications in the materials world *Eur. Polym. J.* **80** 268–94
[10] Meng H and Li G 2013 A review of stimuli-responsive shape memory polymer composites *Polymer* **54** 2199–221
[11] Strankowski M, Piszczyk A, Kosmela P and Korzeniewski P 2015 Morphology and the physical and thermal properties of thermoplastic polyurethane reinforced with thermally reduced graphene oxide *Pol. J. Chem. Technol.* **17** 88–94
[12] Amirian M, Nabipour Chakoli A, Sui J H and Cai W 2013 Thermo-mechanical properties of MWCNT-g-poly (l-lactide)/poly (l-lactide) nanocomposites *Polym. Bull.* **70** 2741–54
[13] Liu J, Wang Z, Li S and Sun X 2019 A novel graphene oxide/trans-1,4-polyisoprene (GO/TPI) shape memory polymer nanocomposite and its multifunctional properties *Nanotechnology* **30** 255706
[14] Sabzi M, Babaahmadi M, Samadi N, G R M, Keramati M and Nikfarjam N 2017 Graphene network enabled high speed electrical actuation of shape memory nanocomposite based on poly(vinyl acetate) *Polym. Int.* **66** 665–71
[15] Babaie A, Rezaei M and Sofla R L M 2019 Investigation of the effects of polycaprolactone molecular weight and graphene content on crystallinity, mechanical properties and shape memory behavior of polyurethane/graphene nanocomposites *J. Mech. Behav. Biomed.* **96** 53–68
[16] Yoonessi M, Shi Y, D A S, Lebron-Colon M, D M T, Weiss R A and Meador M A 2012 Graphene polyimide nanocomposites; thermal, mechanical, and high-temperature shape memory effects *ACS Nano* **6** 7644–55

[17] Sarangapani R, Reddy S T and Sikder A K 2015 Molecular dynamics simulations to calculate glass transition temperature and elastic constants of novel polyethers *J. Mol. Graph. Model.* **57** 114–21
[18] Choi J, Yu S, Yang S and Cho M 2011 The glass transition and thermoelastic behavior of epoxy-based nanocomposites: a molecular dynamics study *Polymer* **52** 5197–203
[19] Wang Y, Wang W, Zhang Z, Xu L and Li P 2016 Study of the glass transition temperature and the mechanical properties of PET/modified silica nanocomposite by molecular dynamics simulation *Eur. Polym. J.* **75** 36–45
[20] Li J, Jin S, Lan G, Chen S and Li L 2018 Molecular dynamics simulations on miscibility, glass transition temperature and mechanical properties of PMMA/DBP binary system *J. Mol. Graph. Model.* **84** 182–8
[21] Lin F, Xiang Y and Shen H 2017 Temperature dependent mechanical properties of graphene reinforced polymer nanocomposites—a molecular dynamics simulation *Composites* B **111** 261–9
[22] Diani J and Gall K 2007 Molecular dynamics simulations of the shape-memory behaviour of polyisoprene *Smart Mater. Struct.* **16** 1575–83
[23] Ghobadi E, Heuchel M, Kratz K and Lendlein A 2013 Simulating the shape-memory behavior of amorphous switching domains of poly(*L*-lactide) by molecular dynamics *Macromol. Chem. Phys* **214** 1273–83
[24] B C A, Liu W K and Keten S 2013 Coarse-grained simulation of molecular mechanisms of recovery in thermally activated shape-memory polymers *J. Mech. Phys. Solids* **61** 2625–37
[25] Zhang X, Yang Q, Liu X, Shang J and Leng J 2020 Atomistic investigation of the shape-memory effect of amorphous poly(*L*-lactide) with different molecular weights *Smart Mater. Struct.* **29** 15040
[26] Moon J, Choi J and Cho M 2016 Programmed shape-dependence of shape memory effect of oriented polystyrene: a molecular dynamics study *Polymer* **102** 1–9
[27] Zhang X, Yang Q and Leng J 2020 How graphene oxide affects shape memory properties and strength of poly(*L*-lactide-co-ε-caprolactone) *J. Intel. Mater. Syst. Struct.* **31** 2152–64
[28] Plimpton S 1995 Fast parallel algorithms for short-range molecular-dynamics *J. Comput. Phys.* **117** 1–19
[29] Sun H 1995 *Ab-initio* calculations and force-field development for computer-simulation of polysilanes *Macromolecules* **28** 701–12
[30] Lu X L, Cai W and Gao Z Y 2008 Shape-memory behaviors of biodegradable poly(*L*-lactide-co-ε-caprolactone) copolymers *J. Appl. Polym. Sci.* **108** 1109–15
[31] Yu Z, Wang Z, Li H, Teng J and Xu L 2019 Shape memory epoxy polymer (SMEP) composite mechanical properties enhanced by introducing graphene oxide (GO) into the matrix *Materials* **12** 1107
[32] Tsai D H 1979 The virial theorem and stress calculation in molecular dynamics *J. Chem. Phys.* **70** 1375–82
[33] Zimmerman J A, Webbiii E B, Hoyt J J, Jones R E, Klein P A and Bammann D J 2004 Calculation of stress in atomistic simulation *Modelling Simul. Mater. Eng.* **12** S319
[34] Keramati M, Ghasemi I, Karrabi M, Azizi H and Sabzi M 2016 Incorporation of surface modified graphene nanoplatelets for development of shape memory PLA nanocomposite *Fiber. Polym.* **17** 1062–8